



Active particle control in the CPD compact spherical tokamak by a lithium-gettered rotating drum limiter

Y. Hirooka^{a,*}, H. Zushi^b, R. Bhattacharyay^c, M. Sakamoto^b, H. Idei^b, T. Yoshinaga^b, Y. Nakashima^d, Y. Higashizono^d, The CPD group^b

^aNational Institute for Fusion Science, Oroshi, Toki, Gifu 509-5292, Japan

^bKyushu University, Kasuga, Fukuoka 816-8580, Japan

^cInterdisciplinary Graduate School of Engineering Science, Kyushu University, Kasuga, Fukuoka 816-8580, Japan

^dUniversity of Tsukuba, Tsukuba, Ibaraki 305-8577, Japan

ARTICLE INFO

PACS:
52.40.Hf
28.52.Fa
28.52.Lf

ABSTRACT

Active particle control capabilities of a lithium-gettered rotating drum poloidal limiter have been demonstrated during 50 kW RF-current drive discharges in a compact spherical tokamak with the major and minor radii of 30 and 20 cm, respectively. The pulse length is typically ~ 300 ms with a flat-top of ~ 250 ms. The rotating limiter is in the shape of cylinder with the diameter and axial length of 15 and 12 cm, respectively. It has reproducibly been observed that, as soon as the rotating drum is gettered with lithium, hydrogen recycling measured with H_α spectroscopy decreases by a factor of ~ 3 not only near the limiter but also in the center stack region. Also, the oxygen impurity level measured with O-II spectroscopy is reduced by a factor of ~ 3 . Meanwhile, the core electron temperature increases from around 7 eV to 20 eV along which the flat-top toroidal plasma current is found to nearly double even at the same vertical magnetic field. Comprehensive surface analysis has been conducted to investigate hydrogen and lithium distributions over the rotating drum after plasma exposure.

© 2009 Elsevier B.V. All rights reserved.

1. Introduction

It is widely recognized in the magnetic fusion community that high-performance core plasmas often favor reduced particle recycling from wall components. A variety of wall conditioning techniques such as boronization have been developed to achieve reduced recycling as well as impurity-controlled conditions. Among all these techniques, lithium pellet injection followed by the formation of lithium coatings on the inboard bumper limiter in TFTR is perhaps most successful in improving the core plasma performance, resulting in a record-long energy confinement time ~ 0.35 s during the final DT-campaign [1]. This effect can best be understood such that lithium absorbs hydrogen until it is fully saturated to form LiH, during which period reduced recycling, i.e. 'passive' wall pumping, is maintained. Since then, lithium has been adopted as a PFM (for plasma-facing material) or as coatings to cover PFCs (for plasma-facing components) in a number of confinement devices, including TdeV [2], FTU [3], TJ-II [4], CDX-U [5], and NSTX [6].

Due to the surface saturation with absorbed and/or implanted particles, the efficacy of wall conditioning by any technique has a finite lifetime, necessitating re-conditioning after a certain number of discharges. Clearly, this is not desirable from the point of view of operating steady state fusion power reactors. To resolve this steady state issue, essentially all the imaginable PFC concepts have been proposed over the past decade. Most of these concepts employ some self-replenishing surface component, either solid or liquid, to provide 'active' wall pumping capabilities. One such concept proposed by Hirooka et al. [7] features a moving-belt made of SiC–SiC fiber fabrics with an in-line getter film deposition system. A series of PoP (for proof-of-principle) experiments have been conducted on this concept with the moving-belt simplified by a laboratory-scale rotating drum [8–10]. Results indicate that not only hydrogen but also helium recycling can be reduced to levels significantly lower than 100% even at steady state, so long as the rotating drum is gettered with lithium.

Encouraged by these successful PoP experiments, a similar but custom-designed rotating drum PFC has been constructed to be used as a poloidal limiter in a compact spherical tokamak: CPD (for the Compact Plasma-wall interactions research Device). Active wall pumping effects on global particle recycling, impurity control, and core plasma properties will be presented in this paper.

* Corresponding author.

E-mail address: hirooka.yoshihiko@nifs.ac.jp (Y. Hirooka).

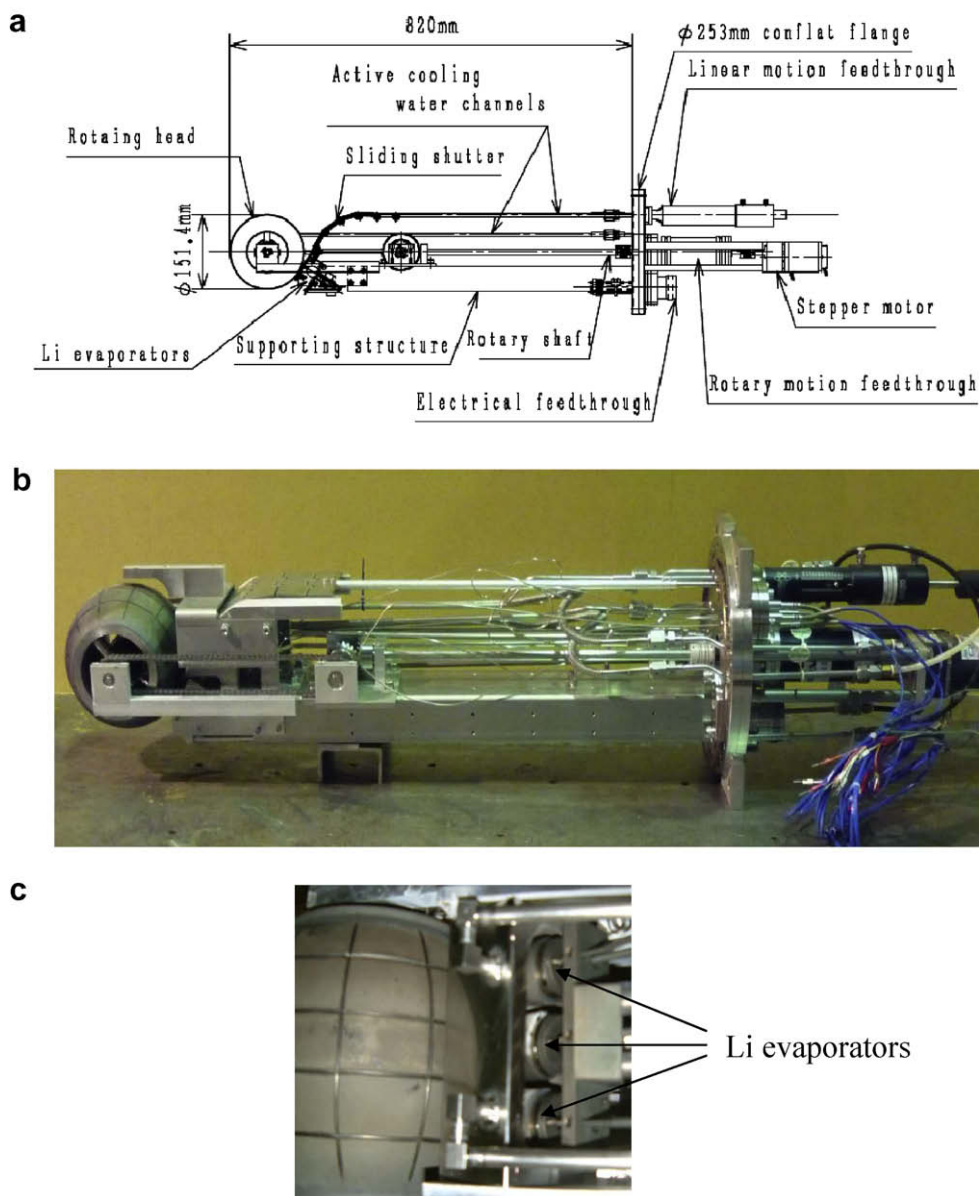


Fig. 1. Rotating drum poloidal limiter for CPD; (a) a blueprint of the rotating drum limiter; (b) a photo of the entire setup; and (c) three lithium evaporators behind the rotating drum after plasma exposure.

2. Experimental

2.1. CPD spherical tokamak

Because details of the CPD spherical tokamak have already been presented elsewhere [11], only technical features important to the present work are described in this section. The major and minor radii are $R_0 = 30$ cm and $a = 20$ cm, respectively. To provide a good access to the vacuum chamber, employed are only four poloidal magnets, which generate a toroidal magnetic field of 0.25 T at $r = R_0$. A cryo-pump with an effective pumping speed of ~ 5200 l/s is employed to prepare vacuum and is kept connected to the CPD chamber to handle exhaust gases during plasma operation. Prior to plasma operation, fuel hydrogen gas is injected through a piezo-electric valve at a flow rate of ~ 0.67 torr l/s for 30 ms. Plasma discharges are then produced by RF current drive in the short pulse mode with an injected power of ~ 50 kW. The plasma dis-

charge duration is typically 300 ms, having a toroidal current flat-top of ~ 250 ms. The flat-top current ranges from 0.3 kA to 1 kA (see Section 3.1 for details). The core plasma density is of the order of 10^{12} ions cm^{-3} , measured by an interferometer, and the electron temperature ranges from 7 eV to 20 eV (see Section 3.1 for details). However, it may be reasonable to assume that ion temperatures are not appreciably different from those associated with the Frank–Condon reaction. The edge plasma density is of the order of 10^{11} cm^{-3} and electron temperature is ~ 5 eV, measured by a Langmuir probe.

2.2. Rotating drum poloidal limiter

The rotating drum poloidal limiter is shown in Fig. 1(a)–(c). The rotating drum is made of water-cooled double-wall stainless steel in the shape of cylinder, the diameter and the axial length of which are ~ 15 cm and ~ 12 cm, respectively. The rotation speed is con-

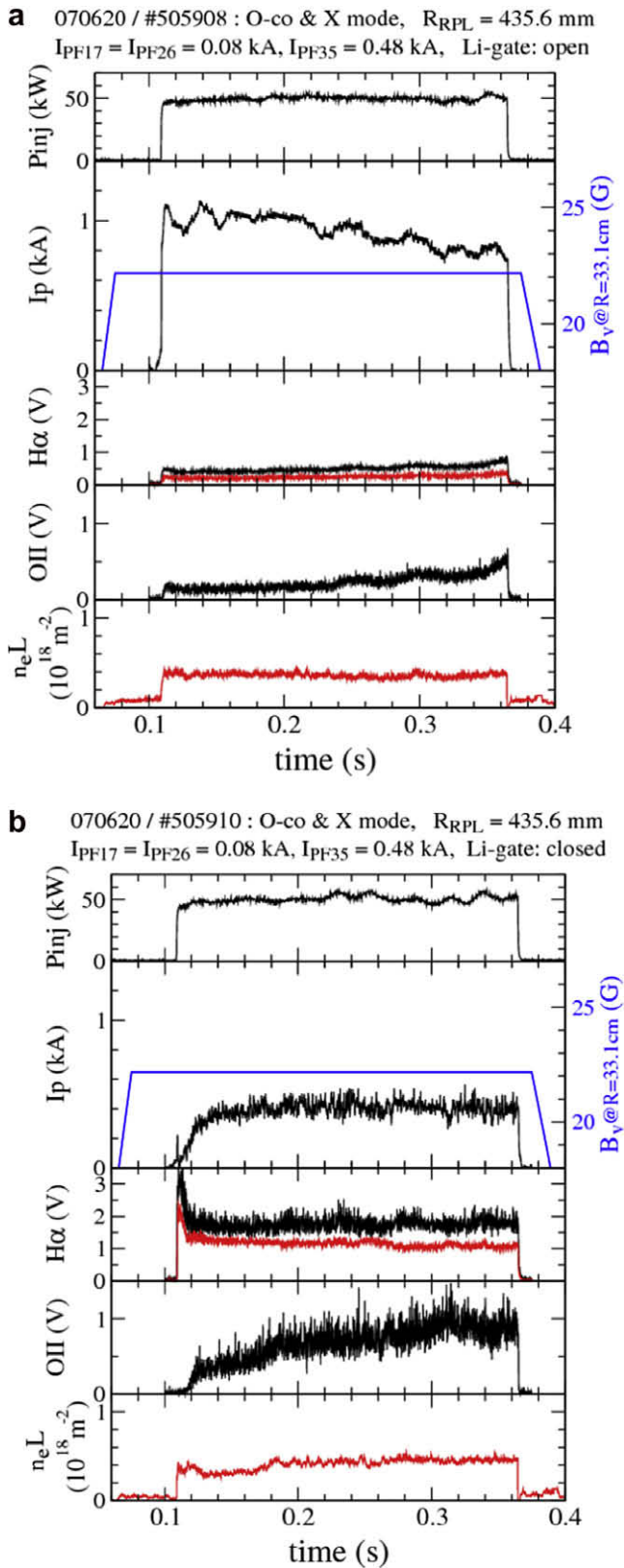


Fig. 2. Wave form data of injected RF power, toroidal current, vertical magnetic field, H_α intensity, O-II intensity, and line-averaged density, taken from a shot (a) with (#505908); and (b) without (#505910) lithium gettering for active wall pumping. For H_α intensity data, the curve in red and black indicate the signals taken near the rotating drum limiter and the center stack, respectively.

trolled by a stepper motor with a chain drive mechanism. The plasma interactive surface is covered with ~ 500 μm thick plasma-

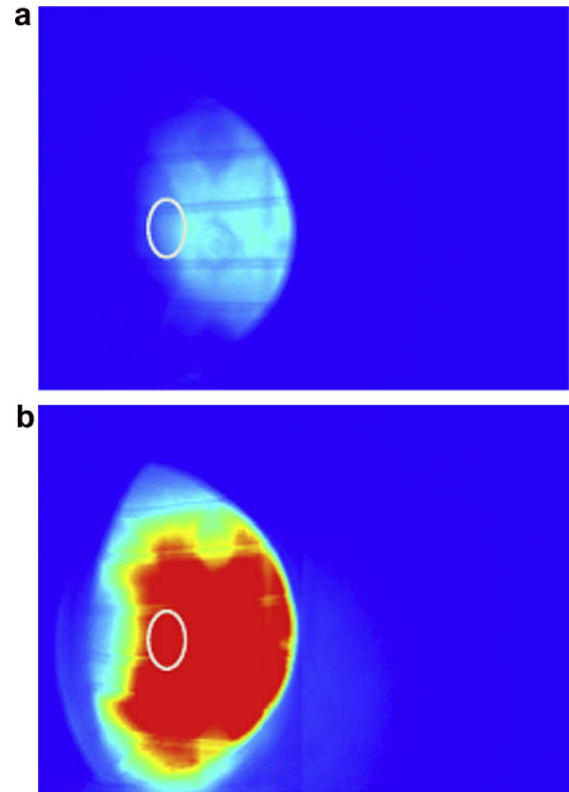


Fig. 3. Tangential CCD camera images of the poloidal plasma cross section through a H_α filter, taken at $t = 200$ ms from a shot (a) with (#505908); and (b) without (#505910) lithium gettering for active wall pumping, where the white open circle shows an approximate position of the rotating drum.

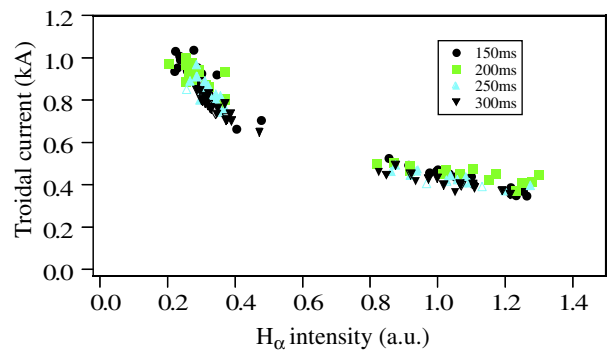


Fig. 4. Relation between the toroidal current and edge H_α intensity. Data are taken at $t = 150, 200, 250,$ and 300 ms from shots #505891 to #505929.

sprayed tungsten coatings, castellated so as to relieve thermal stresses, if any, during plasma exposure. Positioned ~ 10 mm off the rotating drum surface are three lithium evaporators with built-in resistive heaters (see Fig. 1(c) for a close-up), the temperatures of which are monitored individually by thermocouples during gettering operation. A pneumatically operated shutter made of molybdenum is inserted in between the drum surface and these evaporators to control lithium deposition onto the rotating drum. All these components are inserted into a protection structure (shown in Fig. 5(a) as the non-castellated periphery around the rotating drum), which is made of water-cooled copper, but is also coated with plasma-sprayed tungsten similarly to the rotating drum. The entire limiter setup is mounted horizontally from out-board on the torus equator plane, and is moveable linearly for the distance of 5 cm, employing a welded bellows and motorized gear-belt drive mechanism.

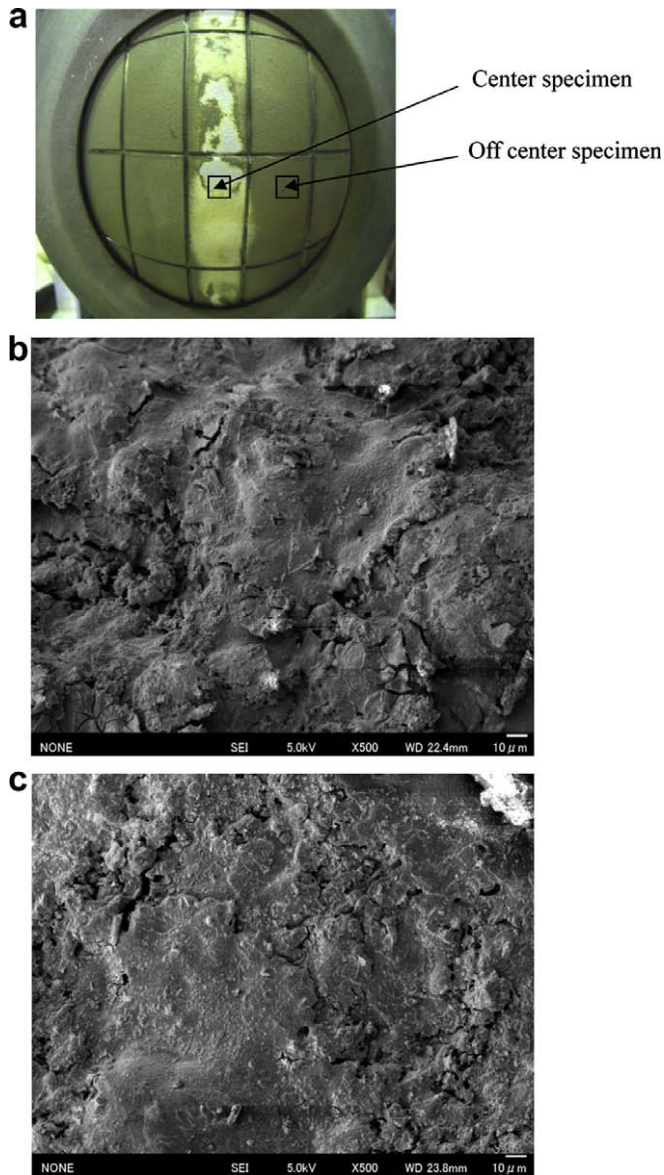


Fig. 5. Macroscopic surface discoloration (a), and scanning electron micrographs taken from specimens cut from the center (b); and off center (c) areas on the rotating drum after two campaigns of lithium gettering and plasma exposure.

2.3. Active particle control campaign

Two separate series of active particle control experiments in CPD were conducted in June 2007 and in July 2007, 135 shots (#505836–505971) and 118 shots (#506792–506910) of ~ 50 kW RF current drive plasma discharges were produced, respectively, using the rotating drum poloidal limiter. In these campaigns, the rotating drum is inserted into the torus in such a way that the inner most drum surface reaches a major radius point of $R = 45.9$ cm. The rotational speed is set at around 4 rpm. First, RF current drive discharges with a relatively low injected power are repeated to condition the surface of plasma-sprayed tungsten without lithium gettering, while the evaporators are gradually heated for thermal outgassing and also for melting loaded lithium. Because the built-in heaters are connected in parallel to a single power supply, for actual lithium gettering, the temperature of the evaporator positioned in the middle (see Fig. 1(c)) is controlled between 400 °C and 420 °C in which range the effective deposition rate onto the rotating drum increases from 2×10^{16} atoms/s/cm² to

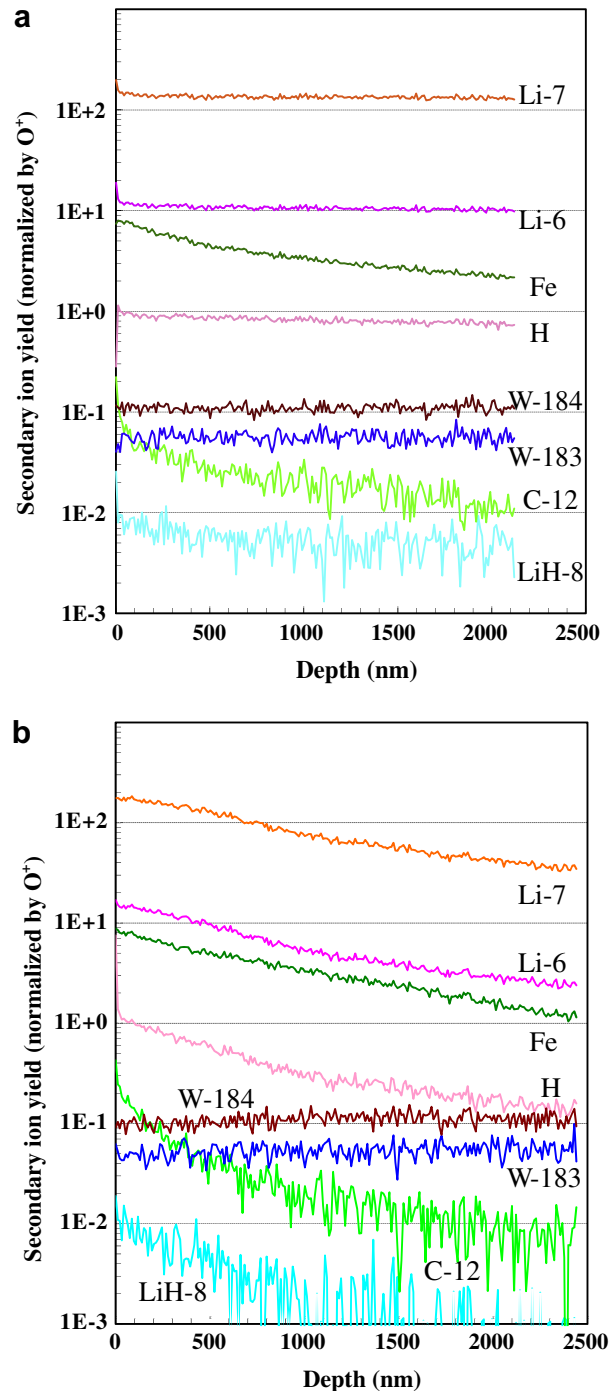


Fig. 6. Secondary ion mass spectrometry data taken from specimens cut from the center (a); and from off center (b) areas on the rotating drum after two campaigns of lithium gettering and plasma exposure.

4×10^{16} atoms/s/cm², estimated from the data taken in our previous work [8]. It is important to mention here that the middle evaporator is typically ~ 20 ° warmer than the others due to heat radiation.

3. Results and discussion

3.1. Active particle control experiments in CPD

Shown in Fig. 2 are the wave form data taken from two shots: #505908 and #505910, both produced in the first campaign with

and without lithium gettering, respectively, in terms of injected RF power, toroidal current, vertical magnetic field, H_α and O-II intensities, line-averaged density. It has reproducibly been observed that, as soon as lithium gettering starts for active wall pumping, the H_α and O-II intensities are reduced by a factor of 2–3 not only in the rotating limiter region but also near the center stack, indicating a global effect as opposed to the local changes seen in our preliminary experiments in which there was no RF-driven toroidal current [11]. These active wall pumping effects are similar to the observations in CDX-U [5] where ohmically heated plasmas are limited by a liquid lithium toroidal ring limiter.

In addition, as shown in Fig. 3, H_α -filtered images taken from these shots during the toroidal current flat-top by a high-speed CCD camera set outboard on the mid-plane, viewing tangentially a poloidal cross-section of the core plasma, exhibit a dramatic difference in depth of penetration by recycling hydrogen. From the toroidal current decay curves (not presented in this paper) after RF power shutdown, the core electron temperatures with and without active wall pumping have been estimated to be ~ 20 and ~ 7 eV, respectively, while in contrast the line-averaged density measured by an interferometer changes only by $\sim 10\%$ (see $n_e L$ data in Fig. 2), similarly to NSTX with passive wall pumping implemented by lithium coatings on the divertor plates [6]. Along with these core property changes, resulting in an increase in plasma pressure as a whole, the toroidal current during the flat-top period is found to nearly double (see I_p data in Fig. 2), which is consistent with a theoretical prediction [12], even at the same vertical magnetic field (see B_v data in Fig. 2). Integrated effects of active wall pumping by the lithium-gettered rotating limiter in CPD are illustrated in Fig. 4, clearly showing a trend that higher toroidal currents favor lower H_α intensity conditions, i.e. lower edge recycling.

3.2. Surface analysis of the rotating drum

Shown in Fig. 5(a) is the rotating drum taken out after two campaigns of active particle control experiments in CPD. One immediately notices a severe surface discoloration which, however, is not the surface damage due to plasma exposure, but is believed to be lithium coatings oxidized up on air exposure. The rotating drum was then cut into pieces for more comprehensive surface analysis with SEM (for scanning electron microscopy), and SIMS (for secondary ion mass spectrometry). Scanning electron micrographs of two specimens (see Fig. 5(a)) are shown in Fig. 5(b) and (c): one cut from the center area in yellowish gray, and the other cut from an off-center area in greenish gray, respectively. Despite the severe discoloration, for both specimens characteristic surface structures of plasma-sprayed tungsten are found remaining, and not so strongly modified in comparison with those before plasma exposure [13]. This is presumably due to the fact that the electron temperature in the edge area in CPD is typically of the order of 5 eV, as mentioned earlier, resulting in relatively low energy ion bombardment.

Results from the SIMS analysis, conducted for the same two specimens as those subjected to SEM, are shown in Fig. 6(a) and (b). A 3 keV oxygen ion (O_2^+) beam is used as the probe at the current density ~ 110 mA/cm². Under these conditions, the silicon-equivalent etching rate is approximately 8 nm/s by which the horizontal axis is converted to depth from elapsed time. Relatively high intensity secondary ions detected are: Li^+ , Fe^+ , H^+ , W^+ , C^+ and LiH^+ with $m/e = 7, 6, 56, 1, 184, 183, 12,$ and 8 , respectively, where m/e is the mass-to-charge ratio. These intensities are normalized by that of O^+ with $m/e = 16$ and plotted as a function of depth. Notice that the Li^+ intensities with $m/e = 6$ and 7 taken from the off-center area (see Fig. 6(b)) decrease more rapidly with increasing depth than those from the center (see Fig. 6(a)). It follows immediately from these data that the drum center is deposited with more lithium than the off-center area, corroborating the discoloration visually observed (see Fig. 5(a)). This is because, as mentioned earlier, the evaporator placed in the middle is warmer than the other two. It is noteworthy that both H^+ and LiH^+ exhibit the same trend as Li^+ in depth distribution. This implies that lithium was hydrogenated as soon as it was deposited for gettering. Also, judging from their depth distributions, Fe^+ and C^+ are considered to be plasma impurities incorporated in lithium deposits.

4. Conclusion

In the present work, a new PFC concept with a 'self-replenishing surface' has been applied to active particle control in a compact spherical tokamak. Results have indicated that hydrogen recycling from the rotating drum limiter as well as in the center stack region is significantly reduced with continuous lithium gettering. Also, oxygen impurity radiation has shown a notable decrease. Combined particle and impurity control effects have led to a significant increase in core electron temperature, and hence in toroidal current as well. All these encouraging data warrant further work on this PFC concept for the development of steady state magnetic fusion devices beyond ITER.

References

- [1] D.K. Mansfield et al., Phys. Plasmas 3 (1996) 1982.
- [2] B. Terreault et al., J. Nucl. Mater. 220–222 (1995) 1130.
- [3] M.L. Apicella et al., J. Nucl. Mater. 363–365 (2007) 1346.
- [4] J.A. Rome (Ed.), Stellarator News, vol. 112, 2007, p. 1.
- [5] R. Majeski et al., Nucl. Fusion 45 (2005) 519.
- [6] H.W. Kugel et al., J. Nucl. Mater. 363–365 (2007) 791.
- [7] Y. Hirooka et al., in: Proceedings of the 17th IEEE-SOFE, San Diego, 6–10 October 1997, p. 906.
- [8] Y. Hirooka et al., Fusion Sci. Technol. 47 (2005) 703.
- [9] Y. Hirooka et al., Nucl. Fusion 46 (2006) 556.
- [10] Y. Hirooka et al., J. Nucl. Mater. 363–365 (2007) 775.
- [11] R. Bhattacharyay et al., Fusion Eng. Design 83 (2008) 1114.
- [12] L.E. Zakharov, G.V. Pereverzev, Sov. J. Plasma Phys. 14 (1988) 75.
- [13] K. Okamoto et al., in: Presented at the 18th International Conference on Plasma–Surface Interactions in Controlled Fusion Devices, Toledo, 26–30 May 2008, J. Nucl. Mater., 390–391 (2009) 671.